A Push–Pull Test To Measure Root Uptake of Volatile Chemicals from Wetland Soils

ARTICLE *in* ENVIRONMENTAL SCIENCE & TECHNOLOGY · MARCH 2013

Impact Factor: 5.33 · DOI: 10.1021/es304748r · Source: PubMed

2 AUTHORS:

Matthew Reid
École Polytechnique Fédérale de Lausanne
15 PUBLICATIONS **62** CITATIONS
SEE PROFILE

Peter R. Jaffe
Princeton University
134 PUBLICATIONS **3,709** CITATIONS
SEE PROFILE

Environmental Science & Technology

Article

pubs.acs.org/est

A Push–Pull Test To Measure Root Uptake of Volatile Chemicals from Wetland Soils

Matthew C. Reid* and Peter R. Jaffé

Department of Civil and Environmental Engineering, Princeton University, Princeton, New Jersey 08544, United States

Supporting Information

ABSTRACT: This paper introduces a novel modification of the single-well "push–pull" test that uses nonvolatile and multiple volatile tracers to investigate the transport and root uptake kinetics of volatile chemicals in saturated soils. This technique provides an estimate of potential volatilization fluxes without relying on enclosure-based measurements. The new push–pull methodology was validated with mesocosm experiments, and bench-scale hydroponic measurements were performed to develop an empirical relationship for scaling root uptake rates between chemicals. A new modeling approach to interpret data using sulfur hexafluoride and helium as dual volatile tracers was developed and shown to decrease errors relative to existing analytical techniques that utilize bromide as a conservative tracer. Root uptake of the volatile tracers was diffusion-limited, and uptake rate constants (k_v) in vegetated experimental mesocosms ranged from 0.021 ± 9.0 × 10^{-4} h^{-1} for CFC-12 to 2.41 ± 0.98 h^{-1} for helium. Hydroponic and mesocosm experiments demonstrate that the molecular diameter is a robust empirical predictor of k_v.

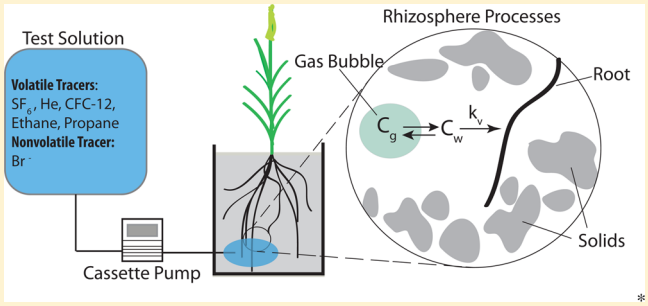

INTRODUCTION

Natural and constructed wetlands are increasingly recognized as low-cost and energy-efficient tools to remove nutrient, trace metal, and organic pollution from water.[1−3] Anaerobic wetland soils are also important sources of trace gases that are detrimental to the environment, including methane (CH_4), nitrous oxide (N_2O), elemental mercury (Hg^0), and methyl halides.[4−6] Because of this key role in the transport and transformation of chemicals, there is active interest in developing in situ techniques to accurately quantify rates of biogeochemical and transport processes in wetland sediments. Plant uptake and volatilization are important transport pathways for trace gases and organic contaminants in wetlands but remain poorly understood and have been incorporated in few predictive models,[7−9] a shortcoming due to both the complexity of the underlying processes and also to the limitations of existing measurement techniques.

Volatilization from wetlands occurs through diffusive exchange across the air–water interface, ebullition of bubbles from near-surface sediments,[10] and transport through vegetation, or phytovolatilization. Plant-mediated transport processes are known to substantially enhance atmospheric fluxes of CH_4[11] and are thought to play similar roles for benzene[12] and Hg^0.[5] Phytovolatilization of CH_4 is limited by root surface area,[13] so chemical uptake processes at the root are key to understanding the mass transport of volatile chemicals along the soil–plant–atmosphere system. Root uptake occurs via a transpiration-driven mechanism[14] and through diffusive exchange between porewater and gas-filled root aerenchyma.[15] The partitioning between these two mechanisms is not clear, but modeling analyses suggest that gaseous diffusion through aerenchyma is the dominant pathway for trace gases such as CH_4, whereas uptake of organic contaminants with lower diffusivities and volatilities is driven by transpiration.[16,17]

In situ quantification of these processes has been hindered by the lack of appropriate measurement techniques. Enclosure-based methods are often used to measure gaseous emissions from soil and provide insight into the transport of volatile chemicals, but are not well-suited to make inferences on rhizosphere processes. Chambers also introduce measurement biases by disturbing meteorological conditions within the chamber and are unable to measure emissions from trees, which are important conduits for both organic pollutants[16,18] and CH_4.[19]

Here we introduce a modified single-well injection withdrawal test, or "push–pull" test (PPT),[20] to make in situ measurements of the transport of volatile chemicals in the wetland rhizosphere and determine root uptake and potential volatilization rates. PPTs involve the injection ("push") of a test solution of reactive and nonreactive tracers into a subsurface porous medium followed by sample extraction ("pull") from the same injection point. First-order reaction rate constants are determined using mass balances of the tracer concentrations in the extracted solution.[21,22] PPTs have been utilized to examine various subsurface biogeochemical processes,[23−25] but to our

Received: November 20, 2012
Revised: February 28, 2013
Accepted: March 5, 2013

   dx.doi.org/10.1021/es304748r | Environ. Sci. Technol. XXXX, XXX, XXX–XXX

knowledge they have not been successfully implemented to quantify uptake kinetics of volatile chemicals or to estimate volatilization rates. We adapt the traditional PPT methodology for these novel measurements by dosing the test solution with volatile tracers and tracking the removal of these tracers from the porewater solution over time.

A volatilization PPT has been proposed previously,[26] but the utility of this earlier approach was limited by the partitioning of the volatile tracer sulfur hexafluoride (SF_6) into subsurface gas bubbles and by the lack of a quantitative framework to scale tracer-derived mass transfer rates to other chemicals. In this contribution, we resolve these problems by developing a dual volatile tracer method that minimizes errors from bubble partitioning and by demonstrating an empirical relationship between uptake rate constants and a chemical's molecular diameter. We use hydroponic batch reactor measurements to investigate interactions between roots and dissolved gases under controlled experimental conditions and to explore the relationship between root uptake and volatilization, and then conduct mesoscale PPTs to validate this new approach in physical models intended to represent field conditions. SF_6, helium (He), dichlorodifluoromethane (CFC-12), ethane, and propane were selected as volatile tracers to span a range of physiochemical properties (Table 1). He and SF_6 are chemically and biologically inert in groundwater.[27,28] Although CFC-12 and the alkanes can be consumed [29] and/or produced [30] in the rhizosphere and roots, control experiments showed that the tracers were stable over the time scales of our measurements.

Table 1. Physiochemical Properties of Volatile Tracers[a]

chemical	K_{aw}[b] (dimensionless)	M^* (g mol^{-1})	log K_{ow}[c] (dimensionless)	σ[d] (Å)
SF_6	150.6	140	1.14	4.71
He	94.5	4	0.28	3.12
CCl_2F_2	17.64	121	2.16	4.86
C_2H_6	19.9	30	1.81	4.28
C_3H_8	28.8	44	2.36	4.75

[a]Parameters are at 25°C. [b]References 31 and 41. [c]References 33, 41, and 49. [d]$\sigma = 0.809V_c^{1/3}$,[47] where V_c is the critical molar volume.[48]

THEORETICAL CONSIDERATIONS

Dissolved Gas Transport in the Presence of Subsurface Bubbles. The "tracer normalization" PPT[21] accounts for the effects of tracer dilution with ambient porewater by normalizing reactive tracer concentrations by the concentration of a nonreactive tracer. Because we use bromide (Br^-) as a nonreactive tracer, we will also refer to this approach as the "bromide normalization" method. Underlying this approach is the assumption that reactive and nonreactive tracers are transported identically, which is not the case for dissolved gases in wetland sediments due to partitioning between water and trapped gas bubbles. This partitioning affects transport as well as measured reaction rates of the volatile tracers but not Br^-.[31,32]

This problem can be accounted for mathematically provided the relative volumes of water-filled (V_w) and gas-filled (V_g) porous medium are known. We modify a derivation presented in Fry et al.[31] by adding a removal term, k_vC, to the 1-D advection–dispersion equation for a nonsorbing, nonreactive dissolved volatile tracer with source/sink terms for bubble-water partitioning:

$$\frac{\partial C}{\partial t} = D\frac{\partial^2 C}{\partial x^2} - \nu\frac{\partial C}{\partial x} - k_v C - \left.\frac{\partial C}{\partial t}\right|_{gw} \quad (1)$$

C is the concentration in the aqueous phase, D is the dispersion coefficient, ν is the velocity of the water, k_v is the removal rate constant [T^{-1}], and $\partial C/\partial t|_{gw}$ is the source/sink term for exchange between the aqueous phase and free gas phases in the soil. We assume equilibrium partitioning of volatile chemicals between water and trapped gas phases and justify this assumption by noting that the time scale for plant uptake (k_v values for SF_6 were measured to be $\sim 10^{-2}$ h^{-1}) is orders of magnitude slower than time scales for bubble-water partitioning, estimated elsewhere to be $\sim 10^{0}$ h^{-1}.[32] Local equilibrium can thus be assumed because the time scale for interphase partitioning is short relative to the time scale of physical uptake by roots.

With the local equilibrium assumption, eq 1 can be simplified to

$$R\frac{\partial C}{\partial t} = D\frac{\partial^2 C}{\partial x^2} - \nu\frac{\partial C}{\partial x} - k_v C \quad (2)$$

R, the retardation factor due to bubble partitioning, is

$$R = 1 + K_{aw}\frac{V_g}{V_w} \quad (3)$$

K_{aw} is the air–water partitioning coefficient. Because hydrodynamic-driven changes are implicitly accounted for in PPTs by tracer normalization, the transport of volatile tracers in the push–pull mesocosms can be described by

$$R\frac{\partial C}{\partial t} = -k_v C \quad (4)$$

Dilution-adjusted volatile tracer concentrations can thus be plotted against time on a natural logarithmic scale, and k_v is given by the slope.[21] This estimate is then multiplied by R to yield a k_v that is corrected for the effects of bubble partitioning. The primary dissolved gas tracers used in these experiments, He and SF_6, are chemically stable and either nonsorbing or very weakly sorbing,[33] so the only plausible loss mechanism is a physical transport process, in this case, uptake by plant roots followed by diffusion through plant biomass to the atmosphere.

The nonpartitioning nature of Br^- is not the only problem associated with its use as a normalizing, conservative tracer for dissolved gases. Br^- is taken up by vegetation and is thus not truly conservative in vegetated sediments,[34] and it cannot be used in marine or estuarine wetlands where background concentrations are high. Because of these limitations, we introduce an alternative method for interpreting dissolved gas PPT data using dual volatile tracers.

Dual Volatile Tracer Approach. The dual volatile tracer technique was adapted from oceanography, where SF_6 and ^{3}He are used to estimate gas transfer velocities in oceans and estuaries using mass balance approaches.[35,36] The relative mass transfer coefficients of the tracers must be known and for open air–water interfaces are given by

$$\frac{v_i}{v_j} = \left(\frac{Sc_i}{Sc_j}\right)^n \quad (5)$$

dx.doi.org/10.1021/es304748r | Environ. Sci. Technol. XXXX, XXX, XXX–XXX

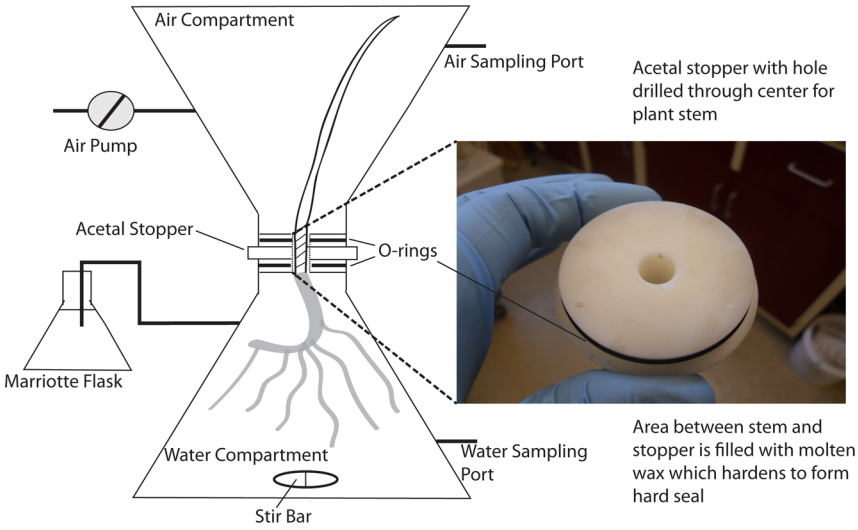

Figure 1. Schematic of hydroponic batch reactor with photo detail of acetal stopper. Drawing is not to scale.

where v is the gas transfer velocity [L T^{-1}] and Sc is the Schmidt number[37] of tracers i and j, respectively. The exponent n varies from $-1/2$ to -1 depending on the turbulence at the air–water interface. The objective of the hydroponic measurements, to be described in the following sections, is to determine whether this relationship is appropriate for modeling root uptake of volatile chemicals or whether an alternative relationship must be developed.

Wanninkhof et al. combine eq 5 with the advection–diffusion equation for two volatile tracers i and j to determine[35]

$$v_i = h\frac{d}{dt}\left(\frac{C_i/C_j}{1-(Sc_i/Sc_j)^n}\right) \quad (6)$$

C_i and C_j are volatile tracer concentrations, and h is the depth of the water column that exchanges with the atmosphere. Applying this approach to saturated soils and assuming that root uptake is the only removal process for nonreactive volatile tracers, eq 6 is divided through by h to yield a root uptake rate constant k_v [T^{-1}]. The equation must also be modified to account for tracer partitioning into bubbles and to reflect an accurate relationship for the uptake rate ratio. Hydroponic and mesocosm measurements will show that the ratio of uptake rate constants from water can be described as a function of the molecular diameter σ (Å):

$$\frac{k_{v,i}}{k_{v,j}} = \left(\frac{\sigma_i}{\sigma_j}\right)^n \quad (7)$$

n was determined empirically to be -8.85 ± 1. The resulting bubble-corrected equation for volatile tracer uptake from soils is thus

$$k_{v,j} = \frac{d}{dt}\left(\frac{R_j \ln C_j - R_i \ln C_i}{1-(\sigma_i/\sigma_j)^{-8.85}}\right) \quad (8)$$

A full derivation of eq 8 is described in the Supporting Information (SI), and the development of eq 7 is detailed under Results and Discussion.

MATERIALS AND METHODS

Hydroponic Batch Reactors. Hydroponic batch reactors were based on a design in ref 14 with the water compartment constructed from a 1.15 L Erlenmeyer flask customized with threaded side arms and an acetal stopper that fit snugly into the mouth of the flask and was sealed with O-rings (Figure 1). The lower 10 cm of a single stem of *Scirpus acutus* (hardstem bulrush) was wrapped in Teflon tape and passed through a hole drilled through the center of the stopper. The stem was held in place with cotton balls, and a heated wax mixture consisting of approximately 20% beeswax, 40% paraffin wax, and 40% petroleum jelly was poured into the hole to create a gastight seal after hardening.[17,38] Control experiments to assess potential leaks or sorption to reactor components or root surfaces were conducted by wrapping a solid glass rod with Teflon tape and securing it in the mouth of the stopper in an identical manner as plant stems. *Scirpus* roots were added to the control's water solution.

The test solution was dosed with the volatile tracers SF_6, He, CFC-12, ethane, and propane using a procedure described in the SI. The hydroponic reactor was filled with the tracer solution and the stopper sealed onto the hydroponic reactor with great care to ensure no formation of headspace or bubbles in the hydroponic solution. One of the side arms served as a sampling port, whereas the other was connected to a constant-head Mariotte flask. Any transpired water was replaced by water from the Mariotte flask, ensuring that no headspace formed in the reactor, allowing for careful accounting of plant water use through gravimetric analysis of the Mariotte flask. The water compartment was continuously mixed with a stir bar. An inverted 4 L flask was fitted to the top of the stopper to create a closed aerial chamber covering the plant. Air was pumped through a desiccant column and through the chamber at a flow rate of approximately 200 mL min^{-1}.

Water samples were collected and analyzed to measure changes in dissolved tracer concentrations. Withdrawal of water from the reactor was carefully tracked so that measurements could be corrected for dilution by "clean" water from the Mariotte flask. To measure static fluxes, the aerial flask was sealed, and six 20 mL discrete air samples were collected over 1 h to determine the accumulation of tracers in the aerial flask. Twenty milliliters of nitrogen gas was introduced to the flask

dx.doi.org/10.1021/es304748r | Environ. Sci. Technol. XXXX, XXX, XXX–XXX

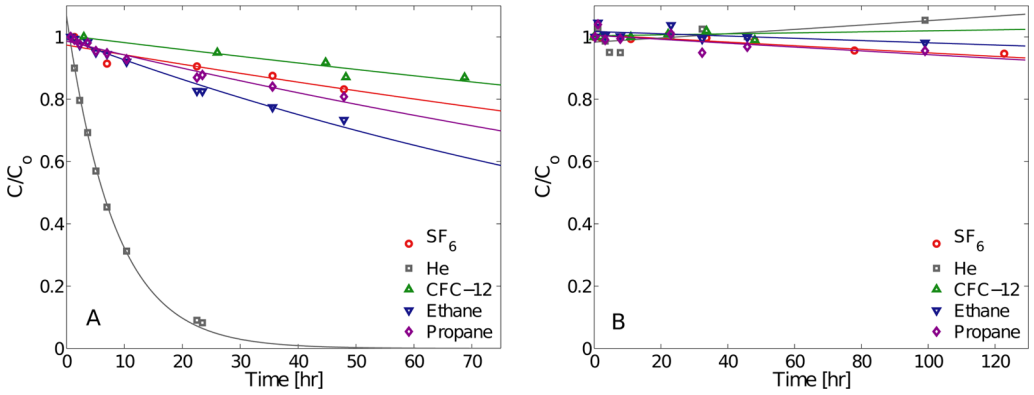

Figure 2. Removal of dissolved volatile tracers from hydroponic reactors with (A) *Scirpus acutus* and (B) sealed control. Symbols are experimental measurements, and lines show model fits to the data, using eq 9. Note the different *x*-axis scales.

prior to the collection of each air sample so as not to create a vacuum in the aerial chamber following withdrawal of air from the fixed-volume flask. Estimation of k_v from static fluxes is described in the SI.

Push–Pull Tests. Mesocosms used for PPTs were based on a design described in ref 17 with the mesocosms in this study having a diameter and depth of 25 cm. The soil was a 1:1 mix of sand and organic topsoil and had a porosity of 0.45. Sampling ports were installed at depths of 3, 7, and 15 cm below the soil surface. Young *S. acutus* and *Typha latifolia* (broad-leaved cattail) were acquired from a commercial nursery and transplanted into mesocosms, with one left unplanted as a control. The plants grew in saturated soil conditions for ~5 months under natural light in a greenhoue before the PPTs were conducted. The mesocosms were moved to an indoor laboratory for PPTs, where they were placed under full-spectrum lamps with 24 h photoperiods.

The test solution was prepared in a 4 L gas-impermeable, collapsible bag, following the procedure used to dose the hydroponic solution. NaBr was added to the solution to yield a Br^- concentration of 7 mM. A peristaltic pump was used to pump the solution through the deepest sampling port into saturated mesocosm soil at a flow rate of 33 mL/min for 15 min. The flexible volume of the bag ensured that no headspace was formed inside the bag as liquid was pumped out. Analysis of the test solution at the beginning and end of the injection phase ensured that there was no leakage of dissolved gases and that the solution was well-mixed. Many push–pull test applications include injection of a "chaser" of deionized water to push the test solution farther into the subsurface medium. We did not include a chaser step because the procedure for estimating the bubble gas volume (see Results) requires the first sample withdrawn in the "pull" phase be at the center of mass of the injected tracer solution. After a resting phase of 30 min, glass syringes were used to withdraw discrete 10 mL water samples from the injection point for tracer analysis. Samples were collected at 0.5–8 h intervals for 2 days following the tracer injection. Note that this push–pull approach uses tracer ratios to infer kinetics in the vicinity of the injection/withdrawal point and, thus, does not provide information on processes at the sediment–air interface.

Sample Collection and Analysis. Dissolved gas tracers were measured using a syringe headspace method[39] with gas chromatography. For PPT samples, an aliquot of the remaining water was placed in a vial for analysis of Br^- with ion chromatography. Details on the syringe headspace method and chromatography are available in the SI.

RESULTS

Hydroponic Batch Reactors. *Water-side Measurements.* The removal of the dissolved gas tracers from a representative hydroponic batch reactor experiment is shown in Figure 2A. The data were fit with a first-order kinetic model:

$$C = C_0\, e^{-k_v t} \tag{9}$$

A nonlinear least-squares regression was used to estimate the parameter k_v. C_0 is the initial concentration and t is time. Results from the nonplant control are shown in Figure 2B and confirm that tracer removal from the planted reactors is due to plant uptake, because the k_v values measured in the control are not significantly different from zero. Losses of tracer mass from the hydroponic solution and accumulation of tracers in the aerial compartment can thus be attributed to transport through plants.

A key variable governing gas exchange between porewater and root aerenchyma is diffusivity,[40] but the diffusion coefficient, D, in the root epidermal layer separating the rhizosphere from aerenchyma is not known. A detailed discussion of gaseous diffusion through root tissues is beyond the scope of this contribution, but if the process is treated analogously to diffusion in aqueous solution, it can be described by the Stokes–Einstein relationship:[41]

$$D = \frac{2kT}{6\pi\eta\sigma} \tag{10}$$

k is the Boltzmann constant, T is temperature, η is the dynamic viscosity of the medium in which diffusion is occurring, and σ is the molecular diameter. Because our measurements were made with multiple tracers in the same hydroponic reactor, the diffusivity ratio of two chemicals, i and j, can be described by

$$\frac{D_i}{D_j} = \left(\frac{\sigma_i}{\sigma_j}\right)^{-1} \tag{11}$$

Figure 3 shows the correlation of k_v with σ^{-1} on log–log axes to test the dependence of k_v on diffusivity. The data were fit with a linear regression, and the slope parameter shows that the k_v ratio can be accurately described by eq 7, with the exponent n determined empirically to be -8.49 ± 0.64.

dx.doi.org/10.1021/es304748r | *Environ. Sci. Technol.* XXXX, XXX, XXX–XXX

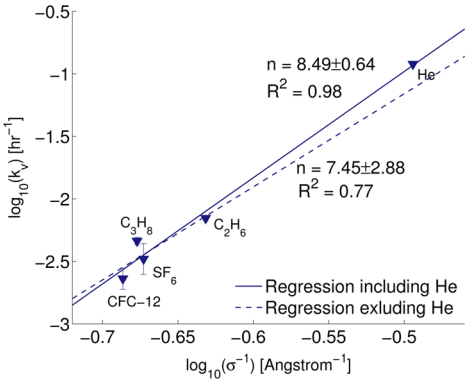

Figure 3. Dependence of hydroponic k_v measurements (▽) on molecular diameter (σ). The slope of the least-squares regression is equal to the exponent n in eq 7, and the uncertainty in n is the standard deviation of the slope parameter. Error bars show ±1 SD of the hydroponic measurements. The regression was performed with and without He to assess whether He, with its small diameter and fast k_v, was biasing the regression analysis.

Air-side Measurements. Figure 4 compares estimates of k_v derived from static fluxes to the aerial chamber with estimates determined from tracer losses from the hydroponic solution, as described in the previous subsection. Rate constants for the removal of He from the hydroponic solution agree well with volatilization rate constants determined with static flux measurements, indicating that He uptake rates from the water are equivalent to rates of volatilization. SF_6 and CFC-12 data indicate that transport of these chemicals through the plant is retarded relative to transport of He.

Push–Pull Tests. Tracer concentrations measured in extracted porewater (SI, Figures S3–S5) reflect the rapid loss of volatile tracers to trapped bubbles in all mesocosms, with planted mesocosms also indicating a longer term removal from porewater due to root uptake. The effect of plants is most clear for He, concentrations of which fall below the detection limit within 5–7 h in both planted mesocosms but remain measurable in the unplanted mesocosm 50 h after injection. The effect of bubbles is seen most clearly with SF_6 in the unplanted control, where concentrations drop significantly within the first 2 h due to partitioning and then remain relatively constant for the remainder of the experiment.

Tracer Normalization Approach. Removal rate constants were determined by normalizing volatile tracer concentrations with Br^- and fitting the log-transformed data with a linear regression (Figure 5A). The slope is equal to $-k_v$.[21] For SF_6 and He, the only removal mechanism is uptake by roots. Whereas there are plausible loss mechanisms for the other volatile tracers, data from the PPT in the unplanted control (Figure 5A, inset) show that all of the tracers exhibit conservative behavior during the 50 h time scale of the experiment, suggesting that losses observed in the vegetated mesocosms are due to the plants and not interactions with soil or bacteria.

The retardation factor R must be determined to correct k_v for the effect of partitioning into bubbles. We use a mass balance approach[42] to quantify the trapped gas volume. The y-intercept of the regression of Br^--normalized concentrations (Figure 5A) is interpreted as the dilution-corrected concentration remaining in aqueous solution following quasi-instantaneous partitioning of gas tracers into bubbles during the injection. The mass of tracer lost to gas phases is calculated using the difference between C_0 and the concentration indicated by the y-intercept. The bubble volume in contact with the injected tracer solution, V_g, is then determined using

$$V_g = \frac{\mathrm{mol}_g V_w}{K_{aw}\mathrm{mol}_w} \tag{12}$$

where V_w is the volume of the injected tracer solution and mol_g and mol_w are the numbers of moles in the gas phase and aqueous phase, respectively. He data are excluded from this analysis because of its extremely fast uptake by roots, but data from the other volatile tracers provide four independent estimates of V_g, which are used to give a mean and standard deviation for V_g/V_w. R is then calculated using eq 3 and is used to produce bubble-corrected k_v values. This analysis yields an estimate of the initial bulk bubble volume, but provides no information on the spatial distribution of bubbles or the evolution of bubble volume over time. Note that estimates of V_g/V_w, and thus of R, are characterized by significant uncertainty, the implications of which will be considered under the Discussion. Results from the tracer normalization analysis are summarized in Table 2.

A log–log plot of bubble-corrected k_v against σ^{-1} (Figure 6) demonstrates a relationship for the k_v ratio that is consistent with that observed in the hydroponic reactors. Regression

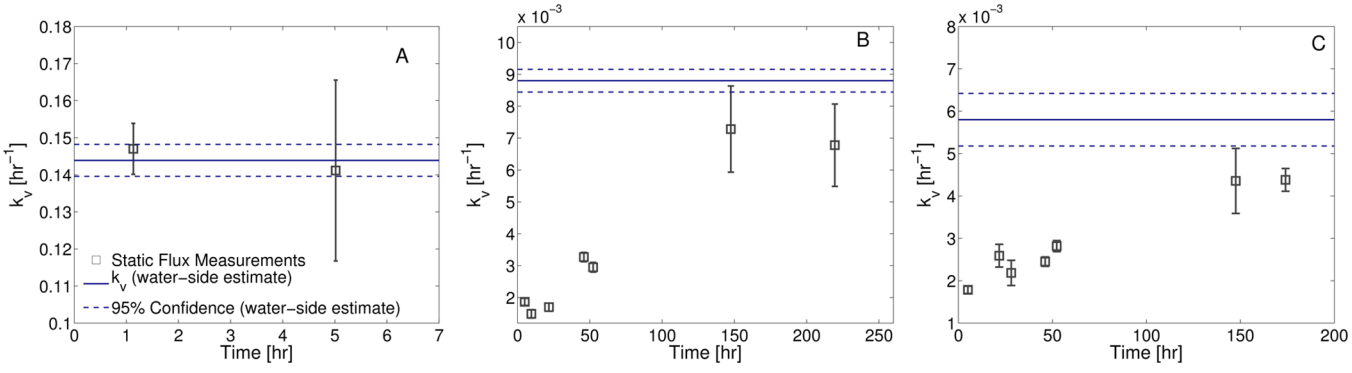

Figure 4. Hydroponic k_v estimates from water-side measurements and from static fluxes (□) to the aerial chamber for (A) He, (B) SF_6, and (C) CFC-12. Solid horizontal lines show the k_v determined by fitting a first-order kinetic model to dissolved tracer measurements; dashed lines give 95% confidence intervals. Error bars show 95% confidence intervals of static flux measurements. Note the different axis scales on each plot. After 5 h, the magnitude of He fluxes was too low to be measured accurately.

dx.doi.org/10.1021/es304748r | Environ. Sci. Technol. XXXX, XXX, XXX–XXX

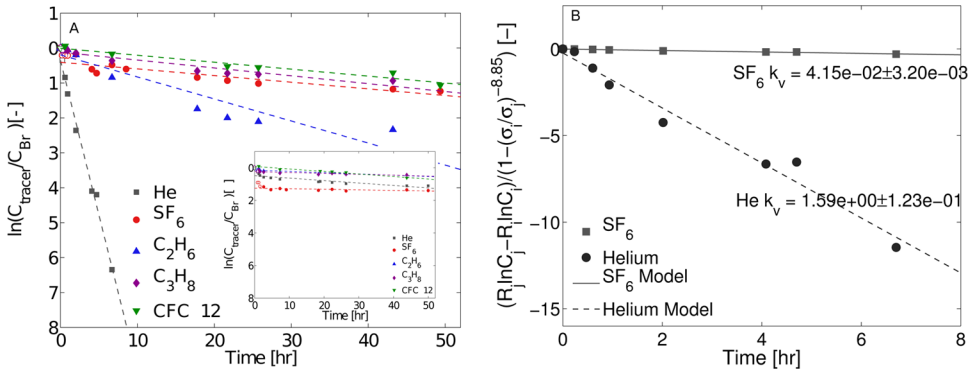

Figure 5. (A) Bromide normalization analysis of PPT results from experiment 3. Symbols show experimental data, and lines show model fits that were used to estimate k_v. The *y*-intercept shows concentrations remaining in solution after quasi-instantaneous partitioning with gas bubbles. The inset shows the results in the unplanted control. (B) Dual volatile tracer analysis of the same data from experiment 3. The subscript *j* refers to the tracer whose k_v is being calculated. All concentrations are expressed as normalized concentrations C/C_0.

Table 2. Parameters Estimated from Mesocosm Push−Pull Tests

					k_v measurement $(h^{-1})^c$	
expt	mesocosm	tracer	V_g/V_w[a]	R^b	tracer−norm[d]	dual tracer
1	unplanted	SF_6	0.0093 ± 0.0038	2.58 ± 0.64	0.0157 ± 0.0043	$1.76 \times 10^{-4} \pm 1 \times 10^{-5}$
		He		1.98 ± 0.4	0.0291 ± 0.007	$6.75 \times 10^{-3} \pm 4.1 \times 10^{-4}$
		CFC-12		1.12 ± 0.048	$0.0171 \pm 9 \times 10^{-4}$	ND
		ethane		1.19 ± 0.076	$0.0092 \pm 7 \times 10^{-4}$	ND
		propane		1.27 ± 0.11	$0.0069 \pm 7 \times 10^{-4}$	ND
2	*Scirpus*	SF_6	0.0142 ± 0.0096	3.41 ± 1.63	0.080 ± 0.038	0.070 ± 0.019
		He		2.50 ± 1.01	2.41 ± 0.98	2.67 ± 0.74
		CFC-12		1.18 ± 0.12	0.028 ± 0.0031	ND
		ethane		1.28 ± 0.19	0.082 ± 0.013	ND
		propane		1.41 ± 0.28	0.039 ± 0.0077	ND
3	*Typha*	SF_6	0.0055 ± 0.0036	1.93 ± 0.61	0.0369 ± 0.0116	0.0415 ± 0.0077
		He		1.58 ± 0.38	1.40 ± 0.34	1.59 ± 0.29
		CFC-12		1.07 ± 0.046	$0.0213 \pm 9 \times 10^{-4}$	ND
		ethane		1.11 ± 0.071	0.0699 ± 0.0047	ND
		propane		1.16 ± 0.10	0.026 ± 0.0024	ND

[a]Mean ± SD determined from gas partitioning test of all volatile tracers except He. [b]Uncertainties determined by propagating uncertainties in V_g/V_w through eq 3. [c]Uncertainties determined by propagating uncertainties in *R* through calculations of k_v. ND, not determined. [d]Corrected for effects of bubble partitioning using *R* estimate in eq 4.

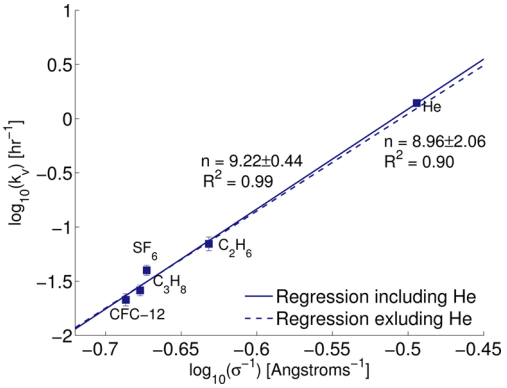

Figure 6. Dependence of push−pull test k_v measurements from experiment 3 (□) on σ. The slope of the least-squares regression estimates the exponent *n* in eq 7, and the uncertainty in *n* is the standard deviation of the slope. Error bars show ±1 SD of the PPT measurements. As with Figure 3, the regression excluding He is used to assess whether He biases the analysis.

analysis shows the exponent *n* in eq 7 is −9.22 ± 0.44, a value that is not statistically different than the one determined from the hydroponic results. The empirical determination of a robust k_v ratio model that is consistent across measurement scales demonstrates that He and SF_6 can be appropriately used together in the dual volatile tracer method.

Dual Volatile Tracer Approach. k_v values for SF_6 and for He were estimated using dual tracer analysis of the same PPT data (Figure 5B), with the exponent *n* assumed to equal −8.85 ± 1 on the basis of an average of the hydroponic and tracer normalization estimates and an uncertainty that conservatively spans the range estimated from each measurement. The retardation factors *R* determined in the tracer normalization approach were used in eq 8. The k_v for SF_6 was computed by setting compound *j* equal to SF_6 and *i* to He, and vice versa for the estimation of the k_v for He. Results are summarized in Table 2.

dx.doi.org/10.1021/es304748r | Environ. Sci. Technol. XXXX, XXX, XXX−XXX

DISCUSSION

Modeling Uptake Rate Constants. The measurements conducted in this study show root uptake of the volatile tracers to be a diffusion-limited process. The dependence of k_v on σ^{-1} in both hydroponic and mesocosm measurements (Figures 3 and 6) is consistent with a dependence on the mass diffusion coefficient, as defined in the Stokes−Einstein relationship to vary inversely with σ. Estimates for the scaling exponent n, estimated to be either -8.49 ± 0.64 or -9.22 ± 0.44, are not predicted by kinetic theory, however, so this result should be regarded as an empirical relationship. This relationship has been validated across different measurement scales, from a well-mixed hydroponic solution to a more realistic saturated organic soil, with a set of chemicals displaying a wide range of physiochemical properties, so it is a robust result.

Note that the dependence of k_v on σ^{-1} does not preclude the possibility of a contribution from a transpiration-driven process, but a mass balance using dissolved tracer concentrations and transpiration rates (described in the SI) shows that a potential transpiration pathway accounts for ≤5% of the uptake in hydroponic experiments and ≤10% of uptake in the mesocosm measurements.

Our conclusion that root uptake of volatile chemicals is diffusion-limited is informed by the selection of tracers employed in this study. Inferences made here should be generalizable to biogenic trace gases such as CH_4, N_2O, and methyl halides due to similarities among properties relevant to gas exchange such as diffusivity and K_{aw}. It is not clear whether these conclusions can be extended to other groups of chemicals such as organic pollutants. Uptake of trichloroethylene by trees is thought to be dominated by the transpiration pathway,[16] for example, and would thus be largely governed by transpiration rates and K_{ow}[8,14] and not diffusion.

Relationship between Uptake and Volatilization. k_v is a rate constant for root uptake of volatile chemicals and is not necessarily equivalent to a volatilization rate constant. For He, the hydroponic measurements showed that the rate constants for uptake and volatilization were the same (Figure 4A). For SF_6 and CFC-12, the uptake rate was higher than the volatilization rate, particularly during the early stages of the experiment (Figure 4B,C), suggesting that transport of these chemicals through the plant was retarded relative to He's. The transport of SF_6 and CFC-12 appears to reach steady state after ∼150 h, at which point volatilization rates come close to matching uptake rates. Sorption to root tissues is a plausible explanation for retarded through-plant transport of the more lipophilic CFC-12 and SF_6 relative to He,[14,43] although root sorption was not measurable in our control experiments (Figure 2B). The disparity between uptake and volatilization rates of SF_6 and CFC-12 thus remains a notable observation with an unclear explanation at this time.

Our results suggest that uptake rates of helium, when scaled to the chemical in question, could provide upper estimates of plant-mediated volatilization rates. Such a "volatilization potential" might be accurate for nonlipophilic chemicals such as CH_4 or N_2O but would likely overestimate volatilization rates of lipophilic chemicals such as chlorinated solvents. This PPT methodology estimates a volatilization potential without relying on flux chambers and could be a useful tool in settings where enclosure-based methods are infeasible. Although this estimate of vegetation-mediated volatilization does not capture diffusive fluxes across the soil surface, plant transport has been shown to be the dominant volatilization pathway for many redox-sensitive trace gases.[44−46]

Comparison of Bromide Normalization and Dual Volatile Tracer Methods. In the planted mesocosms, there was good agreement between the k_v estimates determined with the different analytical approaches to PPT data (Table 2). The dual volatile tracer estimates had smaller uncertainties because the effects of bubble partitioning were already reflected in the measured concentrations of both He and SF_6, and both tracers partition similarly due to their roughly similar K_{aw} values. The "true" volume of trapped bubbles thus has less effect on the final k_v estimates, because the bubbles affect both tracers similarly. In the unplanted control, k_v estimates from the Br^- normalization approach were greater than those from the dual volatile tracer method, particularly for SF_6. We attribute this difference to the bubble partitioning correction (eq 4), in which large bubble fractions can lead to overestimates of k_v. This potential problem again highlights the strength of the dual volatile tracer approach, in which bubble partitioning is implicitly accounted for. Note that the dual volatile tracer approach yields near-zero k_v estimates in the unplanted mesocosm, which is the expected result for the control experiments. The application of the dual volatile tracer method to subsurface processes, which is a central contribution of this work, is thus shown to be an accurate alternative to the Br^- normalization method and can be used in systems in which the use of Br^- as a nonreactive tracer is problematic.

Estimating k_v for Volatile Contaminants. Rate constants for diffusive root uptake of volatile contaminants can be estimated using PPT-derived measurements of tracers such as SF_6 or He and the scaling relationship described in eq 7. The measured k_v for He in experiment 3 can be used with readily available σ parameters[47,48] and eq 7 to estimate a k_v for CFC-12 of 0.028 h^{-1}, whereas the measured value was 0.021 h^{-1}, yielding an error of ∼30%. CFC-12 was selected for this illustrative example because its physiochemical properties are very different from He's and are more similar to those of methyl halides and chlorinated solvents, two groups of volatile chemicals of active environmental interest. In the field, measurements of nonreactive tracers such as He or SF_6 are often preferable to direct measurements of environmental contaminants due to toxicity concerns or the confounding influence of other reactive transport processes that hinder the quantification of a single process. Note that the scaling approach developed here is based on diffusive uptake into gas-filled root aerenchyma and does not account for transpiration-driven processes, so it may underestimate uptake rates for contaminants strongly influenced by transpiration-driven processes.

Error Analysis. Estimates of V_g are characterized by significant errors that affect the calculation of R and thus of k_v. Uncertainties in V_g, taken as the standard deviation of the four V_g estimates determined from the injected gas tracers, were propagated through the calculations of k_v in both the Br^- normalization and dual volatile tracer methods. The results are included in Table 2 and confirm that the dual tracer method estimates k_v with greater precision than the Br^- normalization method.

Other errors result from uncertainty in the exponent n in eq 7. We examine the sensitivity of the prediction of k_v for toluene, whose σ of 5.51 Å is characteristic of organic pollutants, to changes in n (Figure 7). Toluene's k_v was scaled from SF_6 or He k_v measurements using eq 7. The error is computed as the

dx.doi.org/10.1021/es304748r | Environ. Sci. Technol. XXXX, XXX, XXX−XXX

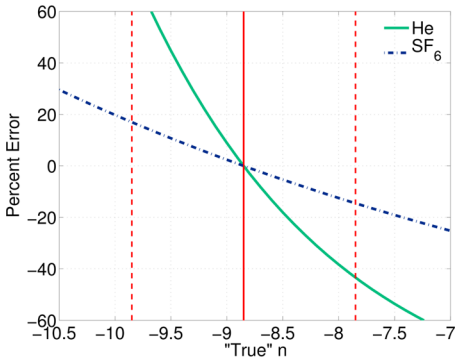

Figure 7. Sensitivity of the k_v estimate for toluene to uncertainty in n, based on extrapolating a PPT-derived k_v of He or SF_6 to toluene. The solid vertical red line shows the best estimate for n with the dashed vertical red lines showing the uncertainty around n. % Error $=100 \times (k_{v,estimate} - k_{v,correct})/k_{v,correct}$.

difference between the prediction determined using $n = -8.85$, the best empirical estimate, and the prediction with a hypothetical "true" n, which was tuned from -7 to -10.5. Underlying this analysis is the assumption that the measurements of SF_6 and He are accurate and that the empirical relationship indicated by Figures 3 and 6 applies to toluene. The estimate based on SF_6 was associated with smaller errors than that based on He because the σ ratio between SF_6 and toluene is smaller than that between He and toluene and, thus, leads to smaller errors in the k_v ratio estimate given uncertainty in n. This analysis indicates that errors in the prediction of k_v for environmental contaminants can be minimized by selecting a tracer with a molecular diameter similar to that of the contaminant in question. The push−pull test methodology introduced here can thus be used with nonreactive dissolved gas tracers such as SF_6 to accurately estimate root uptake rates of volatile environmental contaminants as well as define a potential volatilization rate for these chemicals.

■ ASSOCIATED CONTENT

Supporting Information

Derivation of the modified dual volatile tracer equation, additional details on analytical methods, discussion of the field implementation of the PPT approach, and additional figures. This material is available free of charge via the Internet at http://pubs.acs.org.

■ AUTHOR INFORMATION

Corresponding Author

*E-mail: mcreid@princeton.edu.

Notes

The authors declare no competing financial interest.

■ ACKNOWLEDGMENTS

We thank D. Ho for the generous loan of a GC-TCD and J. Vocaturo and M. Souza for technical assistance. Comments from P. Koster van Groos and three anonymous reviewers greatly improved the quality of the manuscript. This research was funded by NSF CBET - 1133281. M.C.R. acknowledges support from an NSF Graduate Research Fellowship and a New Jersey Water Resources Research Institute Award.

■ REFERENCES

(1) Susarla, S.; Medina, V. F.; McCutcheon, S. C. Phytoremediation: an ecological solution to organic chemical contamination. *Ecol. Eng.* **2002**, *18*, 647−658.
(2) Schnoor, J. L.; Licht, L. A.; McCutcheon, S. C.; Wolfe, N. L.; Carreira, L. H. Phytoremediation of organic and nutrient contaminants. *Environ. Sci. Technol.* **1995**, *29*, 318−324.
(3) Cheng, S.; Grosse, W.; Karrenbrock, F.; Thoennessen, M. Efficiency of constructed wetlands in decontamination of water polluted by heavy metals. *Ecol. Eng.* **2002**, *18*, 317−325.
(4) Bousquet, P.; Ciais, P.; Miller, J.; Dlugokencky, E.; Hauglustaine, D.; Prigent, C. Contribution of anthropogenic and natural sources to atmospheric methane variability. *Nature* **2006**, *443*, 439−443.
(5) Lindberg, S.; Dong, W.; Meyers, T. Transpiration of gaseous elemental mercury through vegetation in a subtropical wetland in Florida. *Atmos. Environ.* **2002**, *36*, 5207−5219.
(6) Rhew, R. C.; Miller, B. R.; Weiss, R. F. Natural methyl bromide and methyl chloride emissions from coastal salt marshes. *Nature* **2000**, *403*, 292−295.
(7) Keefe, S. H.; Barber, L. B.; Runkel, R. L.; Ryan, J. N. Fate of volatile organic compounds in constructed wastewater treatment wetlands. *Environ. Sci. Technol.* **2004**, *38*, 2209−2216.
(8) Dettenmaier, E. M.; Ducette, W. J.; Bugbee, B. Chemical hydrophobicity and uptake by plant roots. *Environ. Sci. Technol.* **2009**, *43*, 324−329.
(9) Seeger, E. M.; Reiche, N.; Kuschk, P.; Borsdorf, H.; Kaestner, M. Performance evaluation using a three compartment mass balance for the removal of volatile organic compounds in pilot scale constructed wetlands. *Environ. Sci. Technol.* **2011**, *45*, 8467−8474.
(10) Vroblesky, D. A.; Lorah, M. M. Prospecting for zones of contaminated ground-water discharge to streams using bottom-sediment gas bubbles. *Ground Water* **1991**, *29*, 333−341.
(11) Sebacher, D. L.; Harriss, R. C.; Bartlett, K. B. Methane emissions to the atmosphere through aquatic plants. *J. Environ. Qual.* **1985**, *14*, 40−46.
(12) Reiche, N.; Lorenz, W.; Borsdorf, H. Development and application of dynamic air chambers for measurement of volatilization fluxes of benzene and MTBE from constructed wetlands planted with common reed. *Chemosphere* **2010**, *79*, 162−168.
(13) Henneberg, A.; Sorrell, B. K.; Brix, H. Internal methane transport through Juncus effusus: experimental manipulaton of morphological barriers to test above- and below-ground diffusion limitation. *New Phytol.* **2012**, *196*, 799−806.
(14) Burken, J. G.; Schnor, J. L. Predictive relationships for uptake of organic contaminants by hybrid poplar trees. *Environ. Sci. Technol.* **1998**, *32*, 3379−3385.
(15) Beckett, P. M.; Armstrong, W.; Armstrong, J. Mathematical modelling of methane transport by *Phragmites*: the potential for diffusion within the roots and rhizosphere. *Aquat. Bot.* **2001**, *69*, 293−312.
(16) Nietch, C. T.; Morris, J. T.; Vroblesky, D. A. Biophysical mechanisms of trichloroethylene uptake and loss in cypress growing in shallow contaminated groundwater. *Environ. Sci. Technol.* **1999**, *32*, 2899−2904.
(17) Reid, M. C.; Jaffe, P. R. Gas-phase and transpiration-driven mechanisms for volatilization through wetland macrophytes. *Environ. Sci. Technol.* **2012**, *46*, 5344−5352.
(18) Ma, X.; Burken, J. G. TCE diffusion to the atmosphere in phytoremediation applications. *Environ. Sci. Technol.* **2003**, *37*, 2534−2539.
(19) Rice, A. L.; Butenhoff, C. L.; Shearer, M. J.; Teama, D.; Rosenstiel, T. N.; Khalil, M. A. K. Emissions of anaerobically produced methane by trees. *Geophys. Res. Lett.* **2010**, *37*, L03807.
(20) Istok, J.; Humphrey, M.; Schroth, M.; Hyman, M.; O'Reilly, K. Single-well, "push-pull" test for in situ determination of microbial activities. *Ground Water* **1997**, *35*, 619−632.
(21) Haggerty, R.; Schroth, H.; Istok, J. Simplified method of "push-pull" test data analysis for determining in situ reaction rate coefficients. *Ground Water* **1998**, *36*, 314−324.

(22) Schroth, M. H.; Istok, J. D. Models to determine first-order rate coefficients from single-well push-pull tests. *Ground Water* **2006**, *44*, 275−283.
(23) Pitterle, M. T.; Andersen, R. G.; Novak, J. T.; Widdowson, M. A. Push-pull tests to quantify in situ degradation rates at a phytoremediation site. *Environ. Sci. Technol.* **2005**, *39*, 9317−9323.
(24) Cho, R.; Schroth, M.; Zeyer, J. Circadian methane oxidation in the root zone of rice plants. *Biogeochemistry* **2011**, *111*, 317−330.
(25) Harrison, M. D.; Groffman, P. M.; Mayer, P. M.; Kaushal, S. S.; Newcomer, T. A. Denitrification in alluvial wetlands in an urban landscape. *J. Environ. Qual.* **2011**, *40*, 634−646.
(26) Amerson, I. L.; Bruce, C. L.; Johnson, P. C.; Johnson, R. L. A multi-tracer push-pull diagnostic test for in situ air sparging systems. *Bioremediation J.* **2001**, *5*, 349−362.
(27) Busenberg, E.; Plummer, L. N. Dating young groundwater with sulfur hexafluoride: natural and anthropogenic sources of sulfur hexafluoride. *Water Resour. Res.* **2000**, *36*, 3011−3030.
(28) Busenberg, E.; Plummer, L. N. Dating groundwater with trifluoromethyl sulfurpentafluoride (SF_5CF_3), sulfur hexafluoride (SF_6), CF_3Cl (CFC-13), and CF_2Cl_2 (CFC-12). *Water Resour. Res.* **2008**, *44*, W02431.
(29) Lovley, D. R.; Woodward, J. C. Consumption of Freons CFC-11 and CFC-12 by anaerobic sediments and soils. *Environ. Sci. Technol.* **1992**, *26*, 925−929.
(30) John, W. W.; Curtis, R. W. Isolation and identification of the precursor of ethane in *Phaseolus vulgaris* L. *Plant Physiol.* **1977**, *59*, 521−522.
(31) Fry, V.; Istok, J.; Semprini, L.; O'Reilly, K.; Buscheck, T. Retardation of dissolved oxygen due to trapped gas phase in porous media. *Ground Water* **1995**, *33*, 391−400.
(32) Vulava, V.; Perry, E.; Romanek, C.; Seaman, J. Dissolved gases as partitioning tracers for determination of hydrogeological parameters. *Environ. Sci. Technol.* **2002**, *36*, 254−262.
(33) Wilson, R. D.; Mackay, D. M. SF_6 as a conservative tracer in saturated media with high intragranular porosity or high organic carbon content. *Ground Water* **1996**, *34*, 241−249.
(34) Xu, S.; Leri, A. C.; Myneni, S. C.; Jaffe, P. R. Uptake of bromide by two wetland plants (*Typha latifolia* L. and *Phragmites australis* (Cav.) Trin. ex Steud. *Environ. Sci. Technol.* **2004**, *38*, 5642−5648.
(35) Wanninkhof, R.; Asher, W.; Weppernig, R.; Chen, H.; Schlosser, P.; Langdon, C.; Sambrotto, R. Gas transfer experiment on Georges Bank using two volatile deliberate tracers. *J. Geophys. Res.* **1993**, *98*, 20237−20248.
(36) Ho, D. T.; Schlosser, P.; Orton, P. M. On factors controlling air-water gas exchange in a large tidel river. *Estuaries Coasts* **2011**, *34*, 1103−1116.
(37) Sarmiento, J.; Gruber, N. *Ocean Biogeochemical Dynamics*; Princeton University Press: Princeton, NJ, 2006.
(38) Briggs, L.; Shantz, H. A wax seal method for determining the lower limit of available soil moisture. *Bot. Gazz.* **1911**, *51*, 210−219.
(39) Wanninkhof, R.; Ledwell, J. R.; Broecker, W. S. Gas exchange on Mono Lake and Crowley Lake, California. *J. Geophys. Res.* **1987**, *92*, 14567−14580.
(40) Armstrong, W.; Cousins, D.; Armstrong, J.; Turner, D.; Beckett, P. Oxygen distribution in wetland plant roots and permeability barriers to gas-exchange with the rhizosphere: a microelectrode and modeling study with *Phragmites australis*. *Ann. Bot.* **2000**, *86*, 687−703.
(41) Schwarzenbach, R.; Gschwend, P.; Imboden, D. *Environmental Organic Chemistry*, 2nd ed.; Wiley: New York, 2003.
(42) Heilweil, V. M.; Solomon, D. K.; Perkins, K. S.; Ellett, K. M. Gas-partitioning tracer test to quantify trapped gas during recharge. *Ground Water* **2004**, *42*, 589−600.
(43) Briggs, G. G.; Bromilow, R. H.; Evans, A. A. Relationships between lipophilicity and root uptake and translocation of non-ionised chemicals by barley. *Pestic. Sci.* **1982**, *13*, 495−504.
(44) Schütz, H.; Conrad, R.; Goodwin, S.; Seiler, W. Emission of hydrogen from deep and shallow freshwater environments. *Biogeochemistry* **1988**, *5*, 295−311.
(45) Kelley, C. A.; Martens, C. S.; W., U., III. Methane dynamics across a tidally flooded riverbank margin. *Limnol. Oceanogr.* **1995**, *40*, 1112−1129.
(46) van der Nat, F.-J. W.; Middelburg, J. T. Effects of two common macrophytes on methane dynamics in freshwater sediments. *Biogeochemistry* **1998**, *43*, 79−104.
(47) Reid, R. C.; Prausnitz, J. M.; Poling, B. E. *The Properties of Gases and Liquids*, 4th ed.; McGraw-Hill: New York, 1987.
(48) Haynes, W. M. *Handbook of Chemistry and Physics*, 93rd ed.; CRC: Boca Raton, FL, 2012.
(49) Kamlet, M. J.; Abraham, M. H.; Doherty, R. M.; Taft, R. Solubility properties in polymers and biological media. 4. Correlation of octanol/water partition coefficients with solvatochromatic parameters. *J. Am. Chem. Soc.* **1984**, *106*, 464−466.